

Shallow-Depth Variational Quantum Hypothesis Testing

Mahadevan Subramanian¹ and Sai Vinjanampathy^{1,2,3,*}

¹*Department of Physics, Indian Institute of Technology Bombay, Powai, Mumbai 400076, India*

²*Centre of Excellence in Quantum Information, Computation, Science and Technology,
Indian Institute of Technology Bombay, Powai, Mumbai 400076, India.*

³*Centre for Quantum Technologies, National University of Singapore,
3 Science Drive 2, Singapore 117543, Singapore.*

(Dated: March 5, 2024)

We present a variational quantum algorithm for differentiating several hypotheses encoded as quantum channels. Both state preparation and measurement are simultaneously optimized using success probability of single-shot discrimination as an objective function which can be calculated using localized measurements. Under constrained signal mode photon number quantum illumination we match the performance of known optimal 2-mode probes by simulating a bosonic circuit. Our results show that variational algorithms can prepare optimal states for binary hypothesis testing with resource constraints. Going beyond the binary hypothesis testing scenario, we also demonstrate that our variational algorithm can learn and discriminate between multiple hypotheses.

Introduction.— Quantum resources have been implied in the enhanced performance of technology tasks in the future such as computing, communication and hypothesis testing. In view of this, the presence of noisy intermediate scale quantum (NISQ) computers presents an opportunity to go beyond algorithms that are classical in nature [1, 2]. Variational quantum algorithms (VQAs) [3, 4] are algorithms that solve optimization problems by evaluating a cost function using a parameterized quantum circuit (PQC) and updating parameters using classical optimization. Though VQAs have a wide array of applications [5–13], their limitations such as barren plateaus in the optimization landscape [14, 15] have sparked discussion on reducing the depth of these circuits, and the use of local observables to avoid them [16]. Hence, shallow-depth circuits (circuits with depth $\mathcal{O}(1)$ or $\mathcal{O}(\log n)$ for n qubits [16]) with a demonstrable advantage are highly sought after.

In this manuscript, we propose a novel application of VQAs by demonstrating that shallow depth circuits can be employed for performing quantum channel discrimination. We apply our algorithm to the problem of quantum illumination [17–23], where we show that low-depth parameterized quantum circuits (PQCs) can obtain known optimal values for Chernoff bound and trace distance in the case of quantum illumination. We begin by establishing results for discrimination between quantum channels on n qubits in the following section and extend our analysis numerically by simulating bosonic modes for quantum illumination.

Variational Quantum Hypothesis Testing.— Our key insight is that shallow depth VQAs can perform binary hypothesis testing of generic quantum channels. We assert that PQCs are able to recover known optima by providing analytical results for arbitrary quantum hypothesis testing (QHT) tasks and numerical simulations for the task of Gaussian quantum illumination. We briefly review channel discrimination, which aims at distinguish-

ing two generic quantum channels $\mathcal{E}_0 : L(\mathcal{H}) \rightarrow L(\mathcal{H})$ and likewise \mathcal{E}_1 using measurements, with the set of linear operators defined as $L(\mathcal{H})$. The null hypothesis H_0 corresponds to \mathcal{E}_0 and the alternate hypothesis H_1 to \mathcal{E}_1 . An input quantum state $\rho \in D(\mathcal{H} \otimes \mathcal{H})$ is sent to one of two channels creating the output states $\rho_i = (\mathcal{E}_i \otimes \mathbb{I})(\rho)$ ($i = 0$ or 1) [24]. Following this, a measurement is performed over these output states using the positive operator-valued measure (POVM) $\{\Gamma, \mathbb{I} - \Gamma\}$ where Γ is a valid POVM element in $L(\mathcal{H} \otimes \mathcal{H})$. The measurement outcome corresponding to Γ is the acceptance criteria for hypothesis H_0 and outcome $\mathbb{I} - \Gamma$ is the acceptance criteria for H_1 . The type-I error (false positive) is defined as $\alpha = 1 - \text{Tr}(\Gamma\rho_0)$ and type-II error (false negative) is defined as $\beta = \text{Tr}(\Gamma\rho_1)$. Moving forward, we optimize the total error probability $(\alpha + \beta)/2$ under the assumption that either channel has equal likelihood to be applied.

In our protocol, one of the two channels is acted on the prepared state ρ following which the outcome of the POVM $\{\Gamma, \mathbb{I} - \Gamma\}$ is used to determine which channel had been applied. Optimal strategies differ based on whether the channel can be applied sequentially or in parallel [25, 26]. In a general parallel strategy [26], one would be discriminating between the maps $\mathcal{E}_0^{\otimes n}$ and $\mathcal{E}_1^{\otimes n}$. We examine a limited parallel strategy where the channel is applied on n copies of the initial state to better study asymptotic behavior. The Holevo-Helstrom result bounds the total error probability for $\rho_0^{\otimes n}$ and $\rho_1^{\otimes n}$. This asymptotically decays exponentially with the exponent determined by the Chernoff bound between ρ_0 and ρ_1 [27, 28]. In the case of symmetric hypothesis testing [29–31], the minimum error probability for a single copy use of the map is $1/2 - \|\mathcal{E}_0 - \mathcal{E}_1\|_{\diamond}/4$ where $\|\mathcal{E}_0 - \mathcal{E}_1\|_{\diamond}$ is the diamond distance between the two channels. This is defined as

$$\|\mathcal{E}_0 - \mathcal{E}_1\|_{\diamond} = \sup_{\rho} (\|(\mathcal{E}_0 \otimes \mathbb{I}_{\mathcal{H}})(\rho) - (\mathcal{E}_1 \otimes \mathbb{I}_{\mathcal{H}})(\rho)\|_1), \quad (1)$$

where $\|A\|_1 = \text{Tr}\sqrt{A^\dagger A}$ is the trace norm. This bound is a direct extension of the Holevo-Helstrom bound [32, 33]. The diamond distance provides a fundamental bound which holds true for all states in $D(\mathcal{H} \otimes \mathcal{H}')$ with $\dim(\mathcal{H}') \geq \dim(\mathcal{H})$ [24] and hence optimizing over states in $D(\mathcal{H} \otimes \mathcal{H})$ is sufficient to reach an optimal probe.

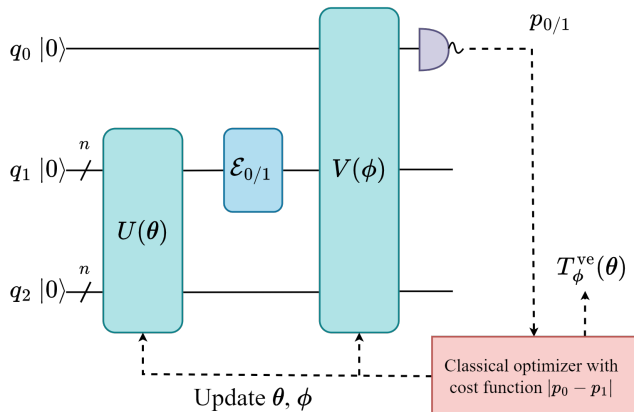


FIGURE 1. Circuit for variational QHT. The state preparation is over the two n qubit registers (or modes) q_1 and q_2 and the map is applied on one mode. An ancillary qubit (or mode) q_0 is used for measurements.

For our variational algorithm, we prepare an entangled probe state ρ_θ in registers q_1 and q_2 using the parameterized unitary $U(\theta)$ as depicted in Fig. 1. This is motivated by the advantage of entangled probe states [24, 34–36] even in the case of entanglement breaking maps [37]. Either the map \mathcal{E}_0 or \mathcal{E}_1 is then applied on the register q_1 . The state after applying the map is $\rho_{i,\theta} = (\mathcal{E}_i \otimes \mathbb{I})(\rho_\theta)$ ($i = \{0, 1\}$).

The optimal protocol is achieved by maximizing the trace distance $\|\rho_{0,\theta} - \rho_{1,\theta}\|_1$, as evidenced from Eq (1) and is known to be difficult [13, 38–40] to evaluate. We get around this by using an estimate of the trace distance as an objective function which makes use of a two-outcome POVM $\{\Gamma, \mathbb{I} - \Gamma\}$. The ancillary qubit q_0 (see Fig. 1) is used for measurements using the parameterized unitary $V(\phi)$ that encodes a Naimark extension [41] of the POVM $\{\Gamma, \mathbb{I} - \Gamma\}$. The probability for outcome Γ is $p_i = \text{Tr}(\Gamma \rho_{i,\theta}) = \text{Tr}((|0\rangle\langle 0| \otimes I)V(\phi)(|0\rangle\langle 0| \otimes \rho_{i,\theta})V(\phi)^\dagger)$. Outcome Γ is the acceptance criteria for hypothesis H_0 and $\mathbb{I} - \Gamma$ is the acceptance criteria for hypothesis H_1 . Hence, $(p_0 + 1 - p_1)/2$ corresponds to the success probability in the classification task. We define a variational estimate of the trace distance $T_\phi^{\text{ve}}(\theta)$, which is always bounded above by the true trace distance and this bound is saturated when $V(\phi)$ encodes a Naimark extension of the Helstrom POVM [13]. The variational estimate of the

trace distance is defined as

$$T_\phi^{\text{ve}}(\theta) = |p_0 - p_1| \leq \frac{1}{2} \|\rho_{0,\theta} - \rho_{1,\theta}\|_1. \quad (2)$$

Our algorithm updates parameters to maximize $T_\phi^{\text{ve}}(\theta)$. $T_\phi^{\text{ve}}(\theta)$ is evaluated with a certain value of θ and ϕ using the quantum computer. These values are then fed into a classical optimizer which proposes updated parameter values for the next iteration and this is repeated till the convergence condition for $T_\phi^{\text{ve}}(\theta)$ is met, after which the values of θ and ϕ are reported. The optimization aims to approach $\theta_0, \phi_0 = \text{argmax}_{\theta, \phi}(T_\phi^{\text{ve}}(\theta))$. Maximizing the value of $T_\phi^{\text{ve}}(\theta)$ clearly maximizes the success probability of discrimination.

While $T_\theta^{\text{ve}}(\phi)$ simplifies the optimization of trace distance by replacing true trace distance with T^{ve} , the numerous parameters in the definitions of $U(\theta)$ and $V(\phi)$ may result in sub-optimal results. Suboptimality can arise in two ways, the first of which is that the optimization may fail to find the optimal states even if $U(\theta)$ is expressible enough for the optimal states. The second source of suboptimality could be that though the qubit measurements produce optimal states according to $T_\theta^{\text{ve}}(\phi)$, these optimized probe states might have a small trace distance evaluated by $T(\rho_{0,\theta}, \rho_{1,\theta})$. The second source of suboptimality is different from the first since an expressible $U(\theta)$ is unrelated to the expressibility of $V(\phi)$, which is simultaneously required to ensure that the “good states are recognized”.

We now proceed to prove that if $U(\theta)$ and $V(\phi)$ are sufficiently expressible, the optimal states generated by the VQAs indeed optimize the real trace distance. This is to verify that our shallow depth circuits are sufficiently expressible for both state preparation and the measurements needed for hypothesis testing. To see this, consider a fixed $U(\theta)$ which generates a (perhaps) sub-optimal state, and then consider the optimization of $V(\phi)$. Since $V(\phi)$ represents the Naimark extension for an ideal two-outcome POVM, if $V(\phi)$ is expressible enough, then it is guaranteed that the optimization of $T_\theta^{\text{ve}}(\phi)$ converges to the real trace distance $T(\rho_{0,\theta}, \rho_{1,\theta})$ (further discussed in the supplemental information [42], which includes references [43–49]). If $U(\theta)$ is expressible, then the globally optimal states are expressible by the VQA. Judging the requirements on the expressibility of $U(\theta)$ can be done by considering the state preparation to occur using a control pulse $\gamma(t)$ which can be represented as b_γ classical bits. If the ideal probe state is reachable in polynomial time and we prepare $\rho_{\theta'}$ such that $\|\rho_{\theta'} - \rho_{\theta_0}\| \leq \epsilon$, the true trace distance $T(\rho_{0,\theta'}, \rho_{1,\theta'}) \in [d(1 - \epsilon), d]$ where $d = T(\rho_{0,\theta_0}, \rho_{1,\theta_0})$ is the maximal trace distance. We know [50] that b_γ scales with $\log(1/\epsilon)$ and the dimension of the manifold of polynomial time reachable states and this gives us an estimate of how much information is needed for having a good state preparation (see [42] for further details). This completes the analysis that our

VQAs can indeed theoretically find the optimal states and measurements to perform the hypothesis test. We now apply our ideas to the example of Gaussian variational quantum illumination to show a practical application of this theoretical result.

Gaussian Variational Quantum Illumination.—Quantum illumination [17–23] is the task of using entangled light to find out if a weakly reflective beam-splitter is present in a bright thermal bath. The map acting on a two-mode bosonic state ρ_{SI} is given as $\mathcal{E}_\eta(\rho_{SI}) = \text{Tr}_S(U_\eta(\rho_B \otimes \rho_{SI})U_\eta^\dagger)$ where $U_\eta = \exp\left(i\sin^{-1}(\eta)(a_S^\dagger a_B - a_S a_B^\dagger)\right) \otimes \mathbb{I}_I$ and ρ_B is the thermal state with an average of N_B photons. The hypothesis H_0 corresponds to the object being absent or equivalently beam-splitter has zero reflectivity hence is the map $\mathcal{E}_{\eta=0}$, and the hypothesis H_1 corresponds to the object being present with some weak reflectivity r hence is the map $\mathcal{E}_{\eta=r}$. Despite clearly being an entanglement breaking map, there is an advantage in using a signal-idler entangled state as first demonstrated in [17]. This advantage holds true even in the limit of $N_B \gg N_S$ where N_S is the average number of signal photons [18, 19].

The probe’s performance is judged by constraining the

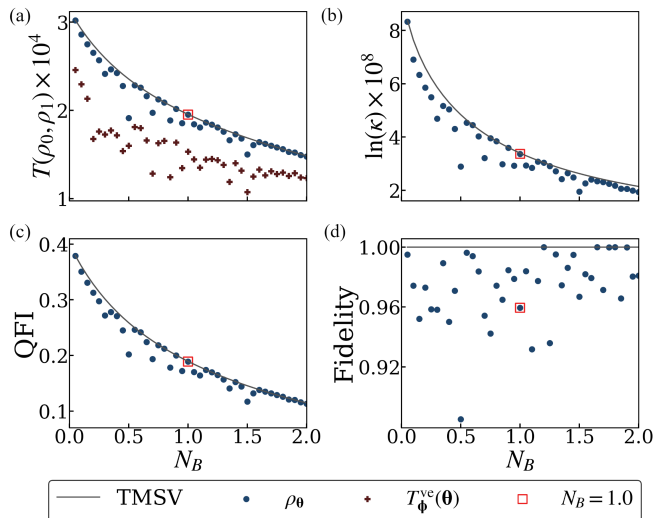


FIGURE 2. Simulation results with constraints mentioned in the main text. Subfigure (a) compares trace distance (blue dots are true trace distance and brown symbols are estimated trace distance), (b) compares Chernoff bound of the optimized state to TMSV, (c) compares QFI and (d) shows fidelity of the optimized state to TMSV. The red square represents shows an inequivalent optimized state with performance equivalent to the TMSV.

average signal photon number to be N_S . This relates the error probability to the energy constrained diamond norm [51]. All the results in this section are in the regime of a signal mode having a constrained photon number of N_S . Under this constraint, the optimal probe

for the task of quantum illumination for single-shot discrimination is proven to be the two-mode squeezed vacuum state (TMSV) as shown in [52, 53]. The optimality of this state comes from the fact that it saturates the Chernoff bound [53] as well as the quantum relative entropy [52] making it suitable for both symmetric and asymmetric hypothesis testing. Even when compared to non-Gaussian states such as a photon-added TMSV [54], TMSV remains optimal for fixed N_S . We note that TMSV state is suboptimal for the Helstrom bound [53].

Our circuit for the task of variational quantum illumination follows the same protocol as that described in Fig. 1 with $q_{0/1}$ being identified as bosonic modes signal S and idler I respectively. We parameterize the unitary U as coherent displacements followed by two mode squeezing each by variable parameters and the unitary V as coherent displacements followed by conditional phase gates followed by beam-splitters. When optimised over these resources, we note that our results compare favourably with known optimal results as seen in Fig. 2. All unitary Gaussian transformations are representable in the Bloch-Messiah decomposition [55]. While this is sufficient for complete parameterization for n -mode Gaussian states, we opt for a hardware-efficient ansatz [5] to see the performance of the algorithm in the restricted setting of having U and V both be composed of single mode operations such as displacements followed by limited two-mode operations such as beam-splitters.

The unitary V encodes the Naimark extension of a two outcome POVM by having the vacuum state measurement on mode q_0 correspond to applying a joint POVM on the signal-idler state. One can always construct a unitary transformation acting on $q_0 \otimes q_1 \otimes q_2$ to transform a projective measurement on q_0 to a projective measurement in the space of $q_1 \otimes q_2$ [56]. The procedure to construct unitary transformations using purely Gaussian operations is summarized in the supplemental information [42].

Our simulation (see [42] for code) over bosonic modes

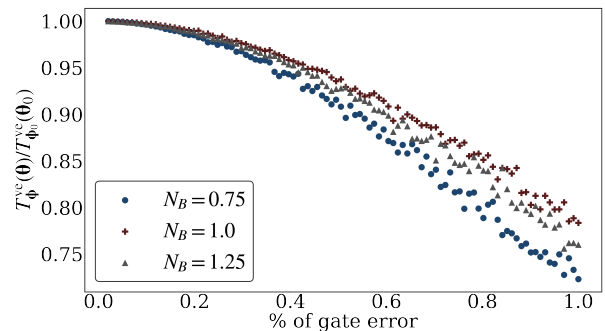


FIGURE 3. Noise robustness of variational quantum illumination showing Gaussian noise variance in gate error against the ratio of $T_\Phi^{\text{ve}}(\theta)$ to the value it takes with zero gate error, optimized with the constraint that $N_S = 0.1$.

[57, 58] maximizes the function $T_{\theta}^{\text{ve}}(\phi)$. In Fig. 2(a) we highlight both the actual trace distance (blue dots) and the estimated trace distance (brown symbols) after optimization. The optimization regularly is able to find the true optimum, in this case given by the TMSV state. Fig. 2(b) shows that the optimality of TMSV for Chernoff bound is nearly matched with our low depth circuit that optimizes $T_{\theta}^{\text{ve}}(\phi)$. This shows that despite optimizing for single-copy discrimination, it is able to optimize to the state which is asymptotically optimal for n copies. Given that the family of maps U_{η} is continuous, our technique can be considered as a quantum sensing task [59]. In the limit of $N_S \rightarrow 0$, the optimal quantum Fisher information (QFI) for this sensing task is given by the TMSV [20]. In Fig. 2(c) we compare the QFI of the optimized state to this optimal value and observe that it is a good quantum sensor input despite being trained for only a fixed value of η . Fig. 2(d) shows that despite reaching near the performance of the TMSV, the optimized states are not exactly equal to the TMSV, implying the existence of a manifold of states that perform just as well as the TMSV. We consider an example with $N_B = 1.0$ (red square) which matches the performance of the TMSV constrained with $N_S = N_I = 0.1$. This state has average photons in idler and signal as $N_I \approx 0.17$ and $N_S = 0.1$ as well as differences in the reduced entropy and the coefficients of the Schmidt decomposition from the TMSV (see the supplemental information [42] for details), demonstrating that it isn't equivalent upto local one mode unitary transformations. To test noise resilience, we plot the averaged objective while the optimized circuit parameters have Gaussian noise (see 3) and find favorable scaling with the error percentage. Our protocol can be trained for in one parameter regime and deployed in another, as discussed in the supplemental information [42]. Additionally, we show a way to construct a near-optimal Gaussian POVM for quantum illumination which supplements existing detection schemes [60].

Multiple Hypothesis Testing.— We can extend the use of our algorithm to the case of multiple channel discrimination [61, 62]. We have quantum channels $\mathcal{E}_1, \mathcal{E}_2, \dots, \mathcal{E}_k$. Extending our earlier description, we now discriminate $\rho_i = (\mathcal{E}_i \otimes \mathbb{I})$ using the POVM set $\{\Pi_1, \dots, \Pi_k\}$. Maximizing the success probability $P_{\text{success}} = \sum_{i=1}^k \text{Tr}(\Pi_i \rho_i) / k$ (assuming each channel to be equally likely) is a semidefinite program over positive semidefinite variables ρ and $\{\Pi_i\}$ with constraints $\text{Tr}(\rho) = 1$ and $\sum_i \Pi_i = \mathbb{I}$. Defining the ancilla q_0 as a qudit with k levels makes it possible to encode a Naimark extension of this POVM set [41]. Proceeding with the same hybrid algorithm described for the binary case, we can now optimize over θ and ϕ to obtain the optimal state and measurement for this task.

We explore a basic case of telling apart three differ-

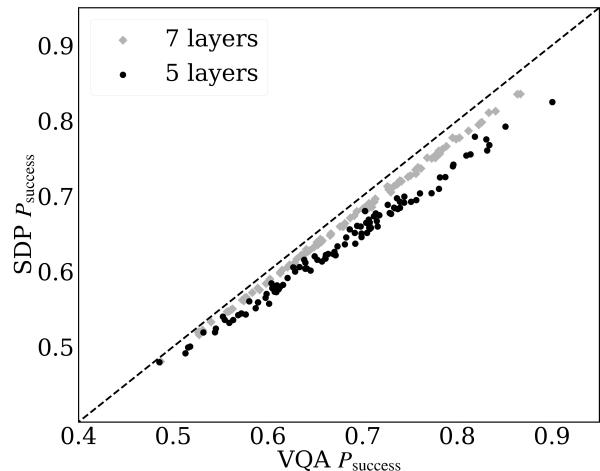


FIGURE 4. Success probability of VQAs for ternary hypothesis test of two-qubit channels over four qubits as described above with a qutrit ancilla. Ansatz $V(\phi)$ (of 5 or 7 layers) is optimized while $U(\theta)$ is fixed and prepares a GHZ state. The VQA outcome is compared against classical SDP result, which can be performed only for small system sizes.

ent 2-qubit unitary channels. There are known analytical results for the multiple state discrimination of asymptotically many copies [63, 64]. However there aren't known results for the case of single-shot discrimination. Hence we compare the performance of our VQA with a convex optimization done using the cvxpy package [65, 66]. Our results are shown in Fig. 4 showing that our algorithm is capable of near optimal performance even in the case of multiple hypotheses.

Discussion.— Hypothesis testing is a task central to probability theory for the discrimination of probability distributions [67]. QHT extends this to quantum channel discrimination and quantum state discrimination, and our work shows how VQAs can be applied for this task. The use of quantum resources have demonstrated an advantage here and have applications in exoplanet spectroscopy [68], superresolution between two incoherent optical sources [69], and as discussed in this work, quantum illumination [17–23]. Our VQA when applied for quantum illumination, is able to find a probe state that matches the optimal performance under signal photon number constraint (see Fig. 2). These results demonstrate noise resilience as shown in Fig. 3 supporting the experimental viability of such algorithms for near-term quantum devices [1, 2].

Our results on QHT have direct application in general channel discrimination [70] and tasks such as quantum reading [71, 72]. It must be noted that the related generalized tasks such as the testing of a quantum channel to be an isometry, the determination of distinguishability between k input states for a quantum channel, or checking equality of two unitaries are QMA-complete [73–75].

We find that the information content of a control pulse required to make the trace distance between the states lie in $[d(1 - \epsilon), d]$ (where d is the maximum possible trace distance between the states obtained on sending a probe state through the channels) scales as $\log(1/\epsilon)$ if the optimal state is polynomially reachable. Hence our algorithm would also take exponential resources to converge for difficult tasks, which situates general complexity-theoretic results within our framework.

Our algorithm nonetheless performs well as benchmarked by channel discrimination measures. The algorithm achieves near optimal results for the discrimination between two-qubit unitaries [42]. Our work can also be clearly generalized to sequential and parallel channel discrimination [26]. These have practical applications in a variety of tasks such as quantum metrology and certifying quantum circuits [76]. We speculate that via the Pinsker's inequality [77] which lower bounds quantum relative entropy in terms of the trace distance, we can generalize our algorithm to asymmetric QHT [78]. Hence variational QHT is sure to find disparate applications in future quantum technologies.

Acknowledgments.— S.V. acknowledges support from Government of India DST-QUEST grant number DST/ICPS/QuST/Theme-4/2019 and thanks Saikat Guha for valuable discussion on discriminating multiple hypotheses.

* sai@phy.iitb.ac.in

- [1] J. Preskill, *Quantum* **2**, 79 (2018).
- [2] K. Bharti, A. Cervera-Lierta, T. H. Kyaw, T. Haug, S. Alperin-Lea, A. Anand, M. Degroote, H. Heimonen, J. S. Kottmann, T. Menke, W.-K. Mok, S. Sim, L.-C. Kwek, and A. Aspuru-Guzik, *Rev. Mod. Phys.* **94**, 015004 (2022).
- [3] M. Cerezo, A. Arrasmith, R. Babbush, S. C. Benjamin, S. Endo, K. Fujii, J. R. McClean, K. Mitarai, X. Yuan, L. Cincio, and P. J. Coles, *Nature Reviews Physics* **3**, 625 (2021).
- [4] J. R. McClean, J. Romero, R. Babbush, and A. Aspuru-Guzik, *New Journal of Physics* **18**, 023023 (2016).
- [5] A. Kandala, A. Mezzacapo, K. Temme, M. Takita, M. Brink, J. M. Chow, and J. M. Gambetta, *Nature* **549**, 242–246 (2017).
- [6] A. Peruzzo, J. McClean, P. Shadbolt, M.-H. Yung, X.-Q. Zhou, P. J. Love, A. Aspuru-Guzik, and J. L. O'Brien, *Nature Communications* **5**, 4213 (2014).
- [7] T. Jones, S. Endo, S. McArdle, X. Yuan, and S. C. Benjamin, *Phys. Rev. A* **99**, 062304 (2019).
- [8] G.-V. Policharla and S. Vinjanampathy, *Phys. Rev. Lett.* **127**, 220504 (2021).
- [9] J. W. Z. Lau, K. H. Lim, K. Bharti, L.-C. Kwek, and S. Vinjanampathy, "Convex optimization for non-equilibrium steady states on a hybrid quantum processor," (2022), [arXiv:2204.03203 \[quant-ph\]](https://arxiv.org/abs/2204.03203).
- [10] R. Kaubruegger, D. V. Vasilyev, M. Schulte, K. Hammerer, and P. Zoller, *Phys. Rev. X* **11**, 041045 (2021).
- [11] C. D. Marciniak, T. Feldker, I. Pogorelov, R. Kaubruegger, D. V. Vasilyev, R. van Bijnen, P. Schindler, P. Zoller, R. Blatt, and T. Monz, *Nature* **603**, 604 (2022).
- [12] J. L. Beckey, M. Cerezo, A. Sone, and P. J. Coles, *Phys. Rev. Research* **4**, 013083 (2022).
- [13] R. Chen, Z. Song, X. Zhao, and X. Wang, *Quantum Science and Technology* **7**, 015019 (2021).
- [14] J. R. McClean, S. Boixo, V. N. Smelyanskiy, R. Babbush, and H. Neven, *Nature Communications* **9**, 4812 (2018).
- [15] S. Wang, E. Fontana, M. Cerezo, K. Sharma, A. Sone, L. Cincio, and P. J. Coles, *Nature Communications* **12**, 6961 (2021).
- [16] M. Cerezo, A. Sone, T. Volkoff, L. Cincio, and P. J. Coles, *Nature Communications* **12** (2021), [10.1038/s41467-021-21728-w](https://doi.org/10.1038/s41467-021-21728-w).
- [17] S. Lloyd, *Science* **321**, 1463 (2008).
- [18] J. H. Shapiro and S. Lloyd, *New Journal of Physics* **11**, 063045 (2009).
- [19] S.-H. Tan, B. I. Erkmen, V. Giovannetti, S. Guha, S. Lloyd, L. Maccone, S. Pirandola, and J. H. Shapiro, *Physical Review Letters* **101** (2008), [10.1103/physrevlett.101.253601](https://doi.org/10.1103/physrevlett.101.253601).
- [20] M. Sanz, U. Las Heras, J. J. Garcia-Ripoll, E. Solano, and R. Di Candia, *Phys. Rev. Lett.* **118**, 070803 (2017).
- [21] L. Fan and M. S. Zubairy, *Phys. Rev. A* **98**, 012319 (2018).
- [22] S.-Y. Lee, Y. S. Ihn, and Z. Kim, *Phys. Rev. A* **103**, 012411 (2021).
- [23] A. Karsa, G. Spedalieri, Q. Zhuang, and S. Pirandola, *Phys. Rev. Research* **2**, 023414 (2020).
- [24] D. Aharonov, A. Kitaev, and N. Nisan, in *Proceedings of the Thirtieth Annual ACM Symposium on Theory of Computing*, STOC '98 (Association for Computing Machinery, New York, NY, USA, 1998) p. 20–30.
- [25] A. W. Harrow, A. Hassidim, D. W. Leung, and J. Watrous, *Phys. Rev. A* **81**, 032339 (2010).
- [26] J. Bavaresco, M. Muraio, and M. T. Quintino, *Phys. Rev. Lett.* **127**, 200504 (2021).
- [27] K. M. R. Audenaert, J. Calsamiglia, R. Muñoz Tapia, E. Bagan, L. Masanes, A. Acín, and F. Verstraete, *Phys. Rev. Lett.* **98**, 160501 (2007).
- [28] M. Nussbaum and A. Szkoła, *The Annals of Statistics* **37**, 1040 (2009).
- [29] K. Li, *The Annals of Statistics* **42** (2014), [10.1214/13-aos1185](https://doi.org/10.1214/13-aos1185).
- [30] F. Hiai and D. Petz, *Communications in Mathematical Physics* **143**, 99 (1991).
- [31] T. Ogawa and H. Nagaoka, *IEEE Transactions on Information Theory* **46**, 2428 (2000).
- [32] A. S. Holevo, *Problemy Peredachi Informatsii* **9**, 3 (1973).
- [33] C. W. Helstrom, *Journal of Statistical Physics* **1**, 231 (1969).
- [34] G. M. D'Ariano, P. Lo Presti, and M. G. A. Paris, *Phys. Rev. Lett.* **87**, 270404 (2001).
- [35] J. Bae, D. Chruściński, and M. Piani, *Phys. Rev. Lett.* **122**, 140404 (2019).
- [36] M. Piani and J. Watrous, *Phys. Rev. Lett.* **102**, 250501 (2009).
- [37] M. F. Sacchi, *Phys. Rev. A* **72**, 014305 (2005).
- [38] G. M. D'Ariano, M. G. A. Paris, and M. F. Sacchi, "Quantum tomography," (2003), [arXiv:quant-ph/0302028 \[quant-ph\]](https://arxiv.org/abs/quant-ph/0302028).
- [39] J. Watrous, "Quantum computational complexity," (2008), [arXiv:0804.3401 \[quant-ph\]](https://arxiv.org/abs/0804.3401).

- [40] R. Agarwal, S. Rethinasamy, K. Sharma, and M. M. Wilde, “Estimating distinguishability measures on quantum computers,” (2021).
- [41] M. M. Wilde, *Proceedings of the Royal Society A: Mathematical, Physical and Engineering Sciences* **469**, 20130259 (2013).
- [42] “Supplemental material.”
- [43] A. Ben-Aroya and A. Ta-Shma, “On the complexity of approximating the diamond norm,” (2009), [arXiv:0902.3397 \[quant-ph\]](#).
- [44] G. Benenti and G. Strini, *Journal of Physics B: Atomic, Molecular and Optical Physics* **43**, 215508 (2010).
- [45] J. Watrous, “Distinguishing quantum operations having few kraus operators,” (2008), [arXiv:0710.0902 \[quant-ph\]](#).
- [46] J. Johansson, P. Nation, and F. Nori, *Computer Physics Communications* **183**, 1760 (2012).
- [47] J. Johansson, P. Nation, and F. Nori, *Computer Physics Communications* **184**, 1234 (2013).
- [48] A. Ferraro, S. Olivares, and M. G. A. Paris, “Gaussian states in continuous variable quantum information,” (2005), [arXiv:quant-ph/0503237 \[quant-ph\]](#).
- [49] M. G. A. Paris, *The European Physical Journal Special Topics* **203**, 61 (2012).
- [50] S. Lloyd and S. Montangero, *Phys. Rev. Lett.* **113**, 010502 (2014).
- [51] A. Winter, “Energy-constrained diamond norm with applications to the uniform continuity of continuous variable channel capacities,” (2017), [arXiv:1712.10267 \[quant-ph\]](#).
- [52] G. De Palma and J. Borregaard, *Phys. Rev. A* **98**, 012101 (2018).
- [53] M. Bradshaw, L. O. Conlon, S. Tserkis, M. Gu, P. K. Lam, and S. M. Assad, *Phys. Rev. A* **103**, 062413 (2021).
- [54] C. Noh, C. Lee, and S.-Y. Lee, “Quantum illumination with non-gaussian states: Bounds on the minimum error probability using quantum fisher information,” (2021).
- [55] G. Cariolaro and G. Pierobon, *Phys. Rev. A* **94**, 062109 (2016).
- [56] F. Buscemi, M. Keyl, G. M. D’Ariano, P. Perinotti, and R. F. Werner, *Journal of Mathematical Physics* **46**, 082109 (2005).
- [57] T. R. Bromley, J. M. Arrazola, S. Jahangiri, J. Izaac, N. Quesada, A. D. Gran, M. Schuld, J. Swinarton, Z. Zabaneh, and N. Killoran, *Quantum Science and Technology* **5**, 034010 (2020).
- [58] N. Killoran, J. Izaac, N. Quesada, V. Bergholm, M. Amy, and C. Weedbrook, *Quantum* **3**, 129 (2019).
- [59] M. Tsang, *Phys. Rev. Lett.* **108**, 170502 (2012).
- [60] J. H. Shapiro, *IEEE Aerospace and Electronic Systems Magazine* **35**, 8 (2020).
- [61] G. Vazquez-Vilar, in *2016 IEEE International Symposium on Information Theory (ISIT)* (IEEE, 2016).
- [62] H. Yuen, R. Kennedy, and M. Lax, *IEEE Transactions on Information Theory* **21**, 125 (1975).
- [63] K. Li, *The Annals of Statistics* **44** (2016), 10.1214/16-aos1436.
- [64] M. R. Grace and S. Guha, *Phys. Rev. Lett.* **129**, 180502 (2022).
- [65] S. Diamond and S. Boyd, *Journal of Machine Learning Research* **17**, 1 (2016).
- [66] A. Agrawal, R. Verschuere, S. Diamond, and S. Boyd, *Journal of Control and Decision* **5**, 42 (2018).
- [67] C. Scott and R. Nowak, *IEEE Transactions on Information Theory* **51**, 3806 (2005).
- [68] Z. Huang, C. Schwab, and C. Lupo, *Phys. Rev. A* **107**, 022409 (2023).
- [69] M. Tsang, R. Nair, and X.-M. Lu, *Phys. Rev. X* **6**, 031033 (2016).
- [70] G. Chiribella, G. M. D’Ariano, and P. Perinotti, *Phys. Rev. Lett.* **101**, 180501 (2008).
- [71] S. Pirandola, *Phys. Rev. Lett.* **106**, 090504 (2011).
- [72] G. Ortolano, E. Losero, S. Pirandola, M. Genovese, and I. Ruo-Berchera, *Science Advances* **7**, eabc7796 (2021).
- [73] B. Rosgen, in *Theory of Quantum Computation, Communication, and Cryptography*, edited by W. van Dam, V. M. Kendon, and S. Severini (Springer Berlin Heidelberg, Berlin, Heidelberg, 2011) pp. 63–76.
- [74] S. Beigi and P. W. Shor, “On the complexity of computing zero-error and holevo capacity of quantum channels,” (2008), [arXiv:0709.2090 \[quant-ph\]](#).
- [75] D. Janzing, P. Wocjan, and T. Beth, *International Journal of Quantum Information* **03**, 463 (2005).
- [76] G. Chiribella, G. M. D’Ariano, and P. Perinotti, *Phys. Rev. Lett.* **101**, 060401 (2008).
- [77] O. Hirota, “Application of quantum pinsker inequality to quantum communications,” (2020).
- [78] G. Spedalieri and S. L. Braunstein, *Phys. Rev. A* **90**, 052307 (2014).

APPENDIX: SHALLOW-DEPTH VARIATIONAL QUANTUM HYPOTHESIS TESTING

Diamond norm estimation

We have two quantum channels $\mathcal{E}_0 : L(\mathcal{H}) \rightarrow L(\mathcal{H})$ and $\mathcal{E}_1 : L(\mathcal{H}) \rightarrow L(\mathcal{H})$ where $L(\mathcal{H})$ is the set of linear operators from Hilbert space \mathcal{H} to \mathcal{H} . We denote subset of $L(\mathcal{H})$ that are density operators as $D(\mathcal{H})$. We proceed on the task of channel discrimination, and as highlighted in the main text, we pick a state $\rho \in D(\mathcal{H} \otimes \mathcal{H})$ as a probe to the map $\mathcal{E}_i \otimes \mathbb{I}_{\mathcal{H}}$ ($i = 0$ or 1) and then use a POVM $\{\Gamma, \mathbb{I} - \Gamma\}$ for classification. We present this as an algorithm for estimation of diamond distance as well.

Using the parameterized circuit shown in Fig. 1 of the letter, we define the state after applying the map as $\rho_{i,\theta} = (\mathcal{E}_i \otimes \mathbb{I})(\rho_{\theta})$ and $p_i = \text{Tr}(\Gamma \rho_{i,\theta})$. If the unitary $V(\phi)$ encodes the Naimark extension of the POVM $\{\Gamma, \mathbb{I} - \Gamma\}$, we obtain $p_i = \text{Tr}((|0\rangle\langle 0| \otimes I)V(\phi)(|0\rangle\langle 0| \otimes \rho_{i,\theta})V(\phi)^\dagger)$. From this we define the cost function in the following equation which is bounded above by the diamond distance since the diamond distance is defined as the supremum of $\|\rho_{0,\theta} - \rho_{1,\theta}\|_1$ over all possible $\rho \in D(\mathcal{H} \otimes \mathcal{H})$.

$$T_{\phi}^{\text{ve}}(\theta) = |p_0 - p_1| \leq \frac{1}{2}\|\rho_{0,\theta} - \rho_{1,\theta}\|_1 \leq \frac{1}{2}\|\mathcal{E}_0 - \mathcal{E}_1\|_{\diamond} \quad (3)$$

Algorithm 1: Variational quantum algorithm to estimate diamond distance

Take input as \mathcal{E}_0 and \mathcal{E}_1 which are CPTP maps from density matrices in \mathcal{H} to density matrices in \mathcal{H} .

Initialize θ and ϕ which are parameters for $U(\theta)$ and $V(\phi)$.

Define convergence condition for cost function $T_{\phi}^{\text{ve}}(\theta)$.

while $T_{\phi}^{\text{ve}}(\theta)$ has not converged **do**

for $\theta_i = \theta + \Delta\theta_i$ and $\phi_i = \phi + \Delta\phi_i$ for some set of $\Delta\theta_i$ and $\Delta\phi_i$ **do**

Run circuit with parameters θ_i and ϕ_i with CPTP map as $\mathcal{E}_0 \otimes \mathbb{I}_n$

Using measurements on q_0 obtain value of p_0 .

Run circuit with parameters θ_i and ϕ_i with CPTP map as $\mathcal{E}_1 \otimes \mathbb{I}_n$

Using measurements on q_0 obtain value of p_1 .

Assign $T_{\phi_i}^{\text{ve}}(\theta_i) = |p_0 - p_1|$

end

Using $T_{\phi_i}^{\text{ve}}(\theta_i)$ update θ and ϕ with a classical optimizer.

Check convergence of $T_{\phi}^{\text{ve}}(\theta)$.

end

Assign estimated diamond norm = $2T_{\phi}^{\text{ve}}(\theta)$

return final values of θ , ϕ and estimated diamond norm.

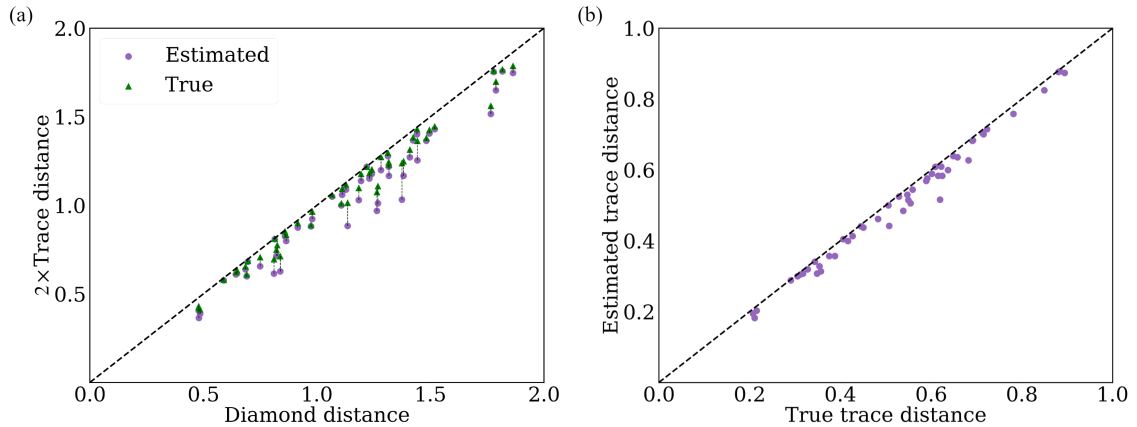


FIGURE 5. Estimation for diamond distance between the identity map and an arbitrary 2 qubit unitary map. (a) Shows how well the value of estimated $T_{\phi}^{\text{ve}}(\theta)$ and the true trace distance $T(\mathcal{E}_0(\rho_{\theta}), \mathcal{E}_1(\rho_{\theta}))$ for the optimized state matches against the analytical value. (b) Shows how well the estimated trace distance matches against the true trace distance for the state ρ_{θ}

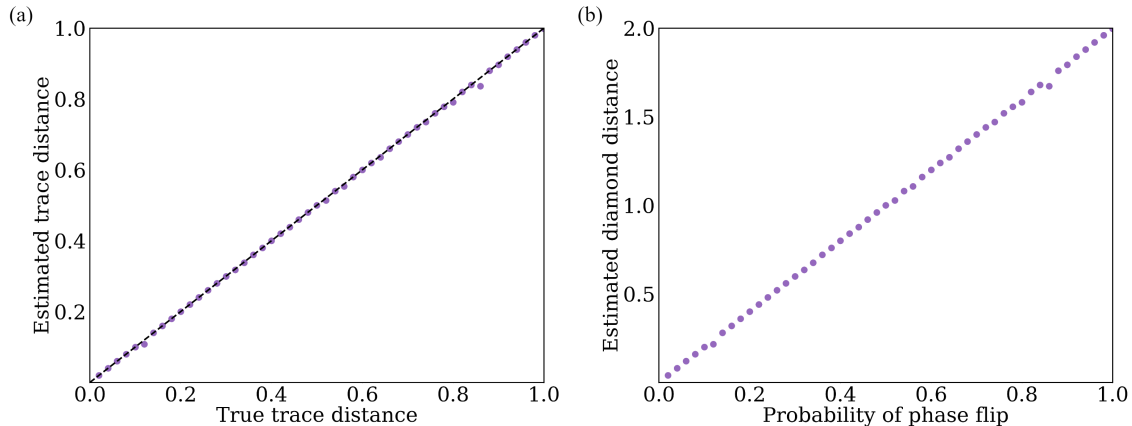


FIGURE 6. Estimation for diamond distance between the identity map and a phase flip map. (a) Shows how well the estimated trace distance matches against the true trace distance for the state ρ_{θ} . (b) Shows the result of the estimated diamond norm against the probability of phase flip.

There are existing ways to find the diamond distance in $\mathcal{O}(\text{poly}(\dim \mathcal{H}))$ since it is a convex optimization problem [43] but this clearly will grow exponentially in size as we increase the number of qubits. Our algorithm is clearly scalable for such situations and can produce results using a hardware efficient ansatz.

Figures 5 and 6 show results of simulations for estimating of diamond norm. The diamond distance between a unitary map and the identity map is the diameter of the circle which is able to contain all the eigenvalues of the unitary operation [44]. For Kraus maps such as the phase flip map of form $\mathcal{E}(\rho) = (1-p)\rho + pZ\rho Z$ have a diamond distance of $2p$ from the identity map [45].

The simulations were carried out using QuTip [46, 47]. The circuit had five qubits with one of them being used in the trace distance estimation subroutine and the other four being used for state preparation after which the quantum map is applied on the first two of the four. The ansatz used was a hardware efficient ansatz [5] where we have single qubit rotations followed by an entangling operation which in this case is made of only CZ gates.

Information content for optimal hypothesis testing

In this section we analyze the minimum amount of information content required for reaching an ϵ -neighbourhood of the state which is optimal for hypothesis testing. This is to understand how much expressibility the ansatz used for state preparation requires to get a sufficiently good probe state. Here we consider the quantum channels $\mathcal{E}_0 : L(\mathcal{H}) \rightarrow L(\mathcal{H})$ and $\mathcal{E}_1 : L(\mathcal{H}) \rightarrow L(\mathcal{H})$ which satisfy the relation $\|((\mathcal{E}_0 - \mathcal{E}_1) \otimes \mathbb{I})\rho_{\text{ideal}}\|_1 = \|\mathcal{E}_0 - \mathcal{E}_1\|_{\diamond} = d$. To be able to reach the state ρ_{ideal} requires providing some classical information which encodes the quantum control problem of approaching this state. We assume that $\rho_{\text{ideal}} \in \mathcal{W}^+$ which is the set of time-polynomial reachable states in $D(\mathcal{H} \otimes \mathcal{H})$ using a certain control scheme $\gamma(t)$ where the set of reachable states are \mathcal{W} . Let there be a state ρ_{real} in the epsilon neighbourhood of ρ_{ideal}

$$\|\rho_{\text{ideal}} - \rho_{\text{real}}\|_1 \leq \epsilon. \quad (4)$$

Using the results of [50], the number of bits which can encode the control pulse $\gamma(t)$ must satisfy

$$b_{\gamma} \geq \dim(\mathcal{W}^+) \log_2 \left(\frac{1}{\epsilon} \right) \quad (5)$$

This can be understood by dividing the space of \mathcal{W}^+ into epsilon balls which would have a volume scaled as $\epsilon^{\dim(\mathcal{W}^+)}$ with respect to the total volume of the space. The information content in $\gamma(t)$ must be enough to specify the epsilon ball which we wish to be in which leads directly to (5). We define the operator $T = (\mathcal{E}_1 - \mathcal{E}_0) \otimes \mathbb{I}$ and the operator norm $\|T\|_1 = \sup_{\rho} \|T\rho\|$ for $\rho \in D(\mathcal{H} \otimes \mathcal{H})$. We can take note of the following from the properties of the diamond

norm [24].

$$\|T\rho_{\text{real}}\|_1 \leq \|T\rho_{\text{ideal}}\| = d \quad (6)$$

$$\|T(\rho_{\text{ideal}} - \rho_{\text{real}})\|_1 \leq \|T\|_1 \|\rho_{\text{ideal}} - \rho_{\text{real}}\|_1 \leq d\varepsilon \quad (7)$$

Using the triangle inequality for the 1-norm we obtain

$$\|T(\rho_{\text{ideal}} - \rho_{\text{real}})\|_1 \geq |\|T\rho_{\text{ideal}}\|_1 - \|T\rho_{\text{real}}\|_1| = d - \|T\rho_{\text{real}}\|_1 \geq 0 \quad (8)$$

Combining the above inequalities, we obtain

$$0 \leq d - \|T\rho_{\text{real}}\|_1 \leq d\varepsilon \implies \|T\rho_{\text{real}}\|_1 \in [d(1 - \varepsilon), d] \quad (9)$$

Notably the minimal b_γ is independent of d . This expression shows that being in the ε neighbourhood of the state which maximizes trace distance implies that the trace distance now lies between $d(1 - \varepsilon)$ and d irrespective of the value of d and will require the same amount of classical information. The computational toughness will arise in the fact that if d is small enough, even the best possible state is unable to tell apart the two channels.

Simultaneous optimization in the algorithm

In this section we will prove that the method of simultaneous optimization employed for the algorithm used for variational quantum hypothesis testing is valid. We first begin with defining the form of our estimated trace distance. There are ways of estimating trace distance using a variational quantum algorithm as shown in [13] and [40]. The main clue lies in the following definition of trace distance.

$$T(\rho_0, \rho_1) = \sup_{P \leq \mathbb{I}} (\text{Tr}(P(\rho_0 - \rho_1))) \quad (10)$$

We can variationally optimize the POVM P to obtain an estimate of the trace distance. To do this using a unitary operation, we must embed the POVM into the unitary operator. For this the Naimark extension can be used [41].

Theorem .1 (Naimark extension). For any POVM $\{\Gamma_i\}_{i \in O}$ acting on a system S , there exists a unitary U_{PS} (acting on a probe system P and the system S) and an orthonormal basis $\{|i\rangle_P\}_{i \in O}$ such that

$$\text{Tr} \left((|i\rangle\langle i| \otimes I_S) U_{PS} (|i\rangle\langle i| \otimes \rho_S) U_{PS}^\dagger \right) = \text{Tr}(\Gamma_i \rho_S) \quad (11)$$

As pointed out in [41], the two-outcome POVM $\{\Gamma, \mathbb{I} - \Gamma\}$ can be encoded in the following unitary with the probe system being a qubit.

$$U_{PS} = \mathbb{I}_P \otimes (\sqrt{\Gamma})_S + i(\sigma_Y)_P \otimes (\sqrt{\mathbb{I} - \Gamma})_S \quad (12)$$

Let us define a parameterized unitary $V(\phi)$ which acts over both the probe and the system. We define the following quantity as an estimate of trace distance,

$$T_\phi(\rho_0, \rho_1) = |p_0 - p_1| \quad (13)$$

$$p_i = \text{Tr} \left((|0\rangle\langle 0| \otimes I) V(\phi) (|0\rangle\langle 0| \otimes \rho_i) V(\phi)^\dagger \right) \quad i \in \{0, 1\} \quad (14)$$

On combining theorem 4.1 and equation (10), we get that $\forall \phi (T_\phi(\rho_0, \rho_1) \leq T(\rho_0, \rho_1))$. This is the main crux of using a variational algorithm for estimating trace distance in [13]. As an extension to this, we define the following cost function for our algorithm where we use an additional qubit as the probe subsystem.

$$T_\phi^{\text{ve}}(\theta) = |p_0(\theta, \phi) - p_1(\theta, \phi)| \quad (15)$$

$$p_i(\theta, \phi) = \text{Tr} \left((|0\rangle\langle 0| \otimes I) V(\phi) (|0\rangle\langle 0| \otimes \mathcal{E}_i(\rho(\theta))) V(\phi)^\dagger \right) \quad i \in \{0, 1\} \quad (16)$$

Our optimization procedure will have to optimize both θ and ϕ for obtaining the best possible state preparation and measurement. Let us define θ_0 and ϕ_0 as follows

$$\theta_0 = \underset{\theta}{\text{argmax}} (\|\mathcal{E}_1(\rho_\theta) - \mathcal{E}_0(\rho_\theta)\|_1) \quad (17)$$

$$\phi_0 = \underset{\phi}{\text{argmax}} (T_\phi^{\text{ve}}(\theta_0)) \quad (18)$$

Here θ_0 optimizes toward the state that saturates the Holevo-Helstrom bound [32, 33]. As per the definition of the optimization problem of trace distance estimation [13], ϕ_0 represents the best parameters to estimate the trace distance for ρ_{θ_0} . Now let us define the parameters obtained by a complete optimization as follows

$$\tilde{\theta}, \tilde{\phi} = \underset{\theta, \phi}{\operatorname{argmax}} (\operatorname{Tr}_{\phi}(\mathcal{E}_1(\rho_{\theta})) - \operatorname{Tr}_{\phi}(\mathcal{E}_0(\rho_{\theta}))) \quad (19)$$

Clearly $T_{\tilde{\phi}}^{\text{ve}}(\tilde{\theta}) \leq \|\mathcal{E}_1(\rho_{\theta_0}) - \mathcal{E}_0(\rho_{\theta_0})\|_1/2$. Our task now would be to verify if $\tilde{\theta}, \tilde{\phi} \equiv \theta_0, \phi_0$, to see whether the global optimization reaches a meaningful result.

Claim .1.1. Under the assumption that for all θ , there exists a ϕ which satisfies

$$T_{\phi}^{\text{ve}}(\theta) = T(\rho_{1,\theta}, \rho_{0,\theta}),$$

we can claim the equivalence $\tilde{\theta}, \tilde{\phi} \equiv \theta_0, \phi_0$.

Proof. From the assumption we have taken, it is quite clear that $T_{\phi_0}^{\text{ve}}(\theta_0) = \|\mathcal{E}_1(\rho_{\theta_0}) - \mathcal{E}_0(\rho_{\theta_0})\|_1$. Along with this, since the parameters $\tilde{\theta}, \tilde{\phi}$ are from an optimization of $T_{\phi}^{\text{ve}}(\theta)$, we must have the following inequality hold

$$T_{\tilde{\phi}}^{\text{ve}}(\tilde{\theta}) \geq T_{\phi_0}^{\text{ve}}(\theta_0)$$

Now from the assumption that we have taken we can make the following claim

$$T_{\tilde{\phi}}^{\text{ve}}(\tilde{\theta}) = \|\mathcal{E}_1(\rho_{\tilde{\theta}}) - \mathcal{E}_0(\rho_{\tilde{\theta}})\|_1$$

If this doesn't hold, there will exist some ϕ which gives the exact trace distance and the TD function always is less than the trace bound hence resulting in a contradiction. Hence we have the following hold

$$\|\rho_{1,\tilde{\theta}} - \rho_{0,\tilde{\theta}}\|_1 \geq \|\rho_{1,\theta_0} - \rho_{0,\theta_0}\|_1$$

Let us assume that $\|\rho_{1,\tilde{\theta}} - \rho_{0,\tilde{\theta}}\|_1 > \|\rho_{1,\theta_0} - \rho_{0,\theta_0}\|_1$. This would contradict the fact that θ_0 is a parameter that saturates the trace distance. Hence we finally get the following hold.

$$\|\rho_{1,\tilde{\theta}} - \rho_{0,\tilde{\theta}}\|_1 = \|\rho_{1,\theta_0} - \rho_{0,\theta_0}\|_1$$

Hence both these parameters saturate the Holevo bound and also they have the perfect trace distance estimators, hence proving their equivalence. \square

While the assumption in the above claim requires $V(\phi)$ to be able to reach the optimal POVM's Naimark extension for all ρ_{θ} , this does show that the optimization procedure is sound and produces meaningful results. In essence, we will have to optimize our estimated trace distance since the real trace distance is not as easy to calculate but this optimization will end up optimizing the true trace distance as well as the estimate of trace distance toward the true value. This has been reflected in the results we show for variational quantum illumination using Gaussian states.

Naimark dilation for Gaussian states

When we are working with purely Gaussian states, we have the limitation that the unitary V must also be a Gaussian unitary. This puts a fundamental limitation on the form it can take, given that no two Gaussian states are orthogonal [48]. The overlap can be made as small as needed, but true orthogonality is impossible and hence we cannot reach the true canonical Naimark extension [49] if we choose to use only Gaussian operations. The isometry of the canonical Naimark extension in this case is given as follows which is not Gaussian.

$$V_{\text{canonical}} = \mathbb{I}_{q_0} \otimes (\sqrt{\Gamma})_{SI} + i(-|0\rangle\langle 1|_{q_0} + |1\rangle\langle 0|_{q_0} + \mathbb{I} - |0\rangle\langle 0| - |1\rangle\langle 1|) \otimes (\sqrt{\mathbb{I} - \Gamma})_{SI} \quad (20)$$

On the other hand, we can frame this as trying to perform a measurement on some n mode state by entangling it to a 1 mode system. This can be written as follows.

$$\operatorname{Tr}(V^\dagger(P_0 \otimes \mathbb{I}_n)V(|0\rangle\langle 0| \otimes \rho)) = \operatorname{Tr}(P\rho) \quad (21)$$

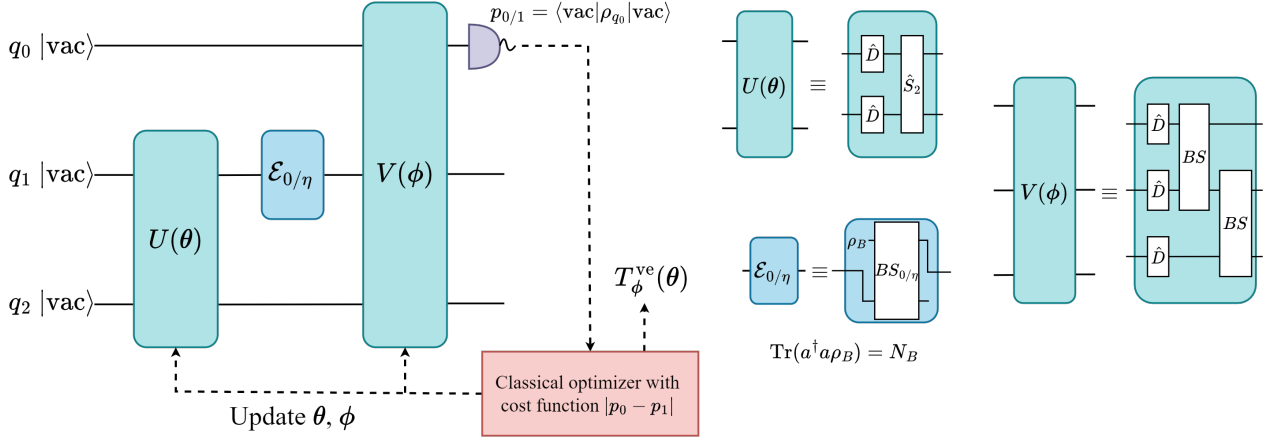


FIGURE 7. Description of the quantum circuit for variational quantum illumination. The state is prepared over the signal and idler mode using an ansatz which consists of displacements and two-mode squeezing. The ansatz shown for the measurement section consists of displacements and beam splitters. The simulations contain controlled phase gates for in the measurement section as well. The readout can be either measure the probability it is vacuum or the expectation value of the parity operator.

Here P_0 is a projection which is in $L(\mathcal{H})$ where \mathcal{H} is the Hilbert space of a single mode of light. P is a projection in $L(\mathcal{H}^{\otimes n})$ and ρ is a density operator in $D(\mathcal{H}^{\otimes n})$ and \mathbb{I}_n is the identity operator in $L(\mathcal{H}^{\otimes n})$. Since we want the above equation to hold for all ρ , we can rewrite it as follows.

$$V^\dagger(P_0 \otimes \mathbb{I}_n)V = \mathbb{I}_1 \otimes P \quad (22)$$

Here we are applying a transformation from one linear operator to another which means that as long as the norm of both $P_0 \otimes \mathbb{I}_n$ and $\mathbb{I}_1 \otimes P$ are equal, we can find a V . We can construct a $V = (\text{SWAP}_{1,2} \otimes \mathbb{I}_{n-1})(\mathbb{I}_1 \otimes V')$ where it performs a swap between the first two modes and then does some unitary V' only on the subsystem of n modes. This transforms the measurement from the space of the first mode to the space of the n modes.

$$(\mathbb{I}_1 \otimes V')^\dagger(\text{SWAP}_{1,2} \otimes \mathbb{I}_{n-1})^\dagger(P_0 \otimes \mathbb{I}_n)(\text{SWAP}_{1,2} \otimes \mathbb{I}_{n-1})(\mathbb{I}_1 \otimes V') = \mathbb{I}_1 \otimes V'^\dagger(P_0 \otimes \mathbb{I}_{n-1})V' \quad (23)$$

This shows that we can construct any projection of form $P = V'^\dagger(P_0 \otimes \mathbb{I}_{n-1})V'$ where V' is Gaussian since the swap operation between two modes can be trivially represented as a passive Gaussian operation. This recipe shows us that while we may not be able to construct the canonical Naimark extension of the optimal POVM, we can construct a Naimark extension that performs a POVM on the n mode subspace using a single-mode ancillary measurement.

Multiple optima in Gaussian quantum illumination

As can be seen in Fig. 2 of the main text, there are certain states which do not have 100% fidelity with the TMSV yet happen to have equal performance in the QFI, chernoff bound and the trace distance. These states are largely accessible due to the constraint only being placed on the value of signal photon number N_S .

We pick the example of the state obtained in the case of $N_B = 1$. We perform a Schmidt decomposition on this state and compare it with the TMSV. Equal Schmidt values imply that one state can be obtained from the other using only local transformations implying equal entanglement as well. It turns out that this is not the case and the TMSV is different from the obtained optimal state despite both being equally good for the hypothesis testing task. This implies that there are clearly multiple possible Gaussian states which are optimal for the hypothesis testing task.

The five largest Schmidt values for TMSV with $N_S = 0.1$ are $6.20921323 \times 10^{-5}$, $6.83013455 \times 10^{-4}$, $7.51314801 \times 10^{-3}$, $8.26446281 \times 10^{-2}$, $9.09090909 \times 10^{-1}$. The TMSV has a von-Neumann entropy of 0.33509970612111517.

The five largest Schmidt values for the obtained optimal state at $N_B = 1$ with $N_S = 0.1$ are $6.03874183 \times 10^{-5}$, $6.69019663 \times 10^{-4}$, $7.41192949 \times 10^{-3}$, $8.21152229 \times 10^{-2}$, $9.09737450 \times 10^{-1}$. This state has a von-Neumann entropy of 0.3332223308457541.

Testing unknown values in variational quantum illumination

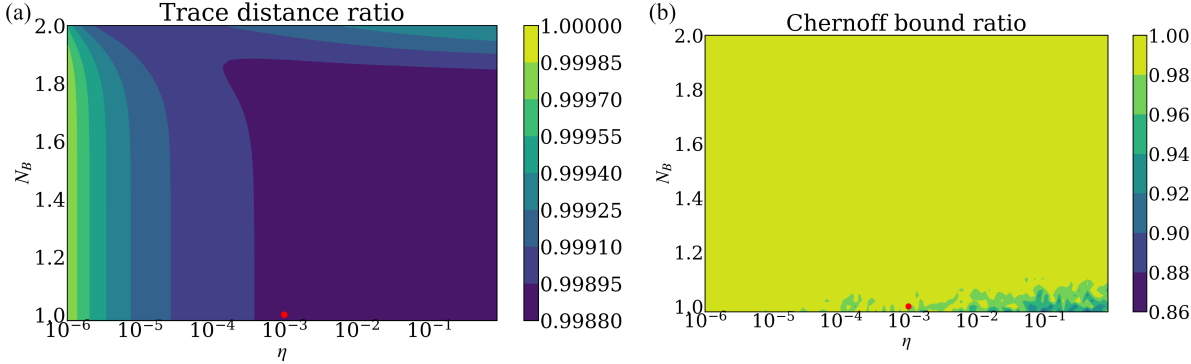


FIGURE 8. Comparison of performance of a specific optimized state over a range of N_B and η . The state we choose is obtained by optimizing with $N_B = 1$ and $\eta = 10^{-3}$ (indicated by a red dot in the image) which as shown previously is quite different from the TMSV. (a) Shows the ratio of trace distance when using the chosen state to that of the trace distance with TMSV. (b) Shows the ratio of Chernoff bound when using the chosen state to that of the trace Chernoff bound with TMSV. Both of these are measures of performance for a good hypothesis test in the symmetric case giving an idea that even over unknown values of N_B and η we obtain states which do perform optimally.

The optimization protocol we use happens to find the optimal state for discriminating two given maps \mathcal{E}_0 and \mathcal{E}_1 . However in the case of quantum illumination, where these maps are dependent on some continuous parameters (background radiation N_B and reflectivity η), one might want to check the applicability of the optimized state for varying values of N_B and η . This is checked by seeing how well a fixed state performs compared to the known optimal TMSV state as can be seen in Fig. 8.

Simulation code and data

All the simulation code and data for variational Gaussian quantum illumination, general QHT, and multiple hypothesis testing can be found here: <https://github.com/mahadevans2432/Variational-QHT>.